

# Catalysis Science & Technology

[www.rsc.org/catalysis](http://www.rsc.org/catalysis)



ISSN 2044-4753



**PAPER**

Wenfeng Shangguan, Adam F. Lee *et al.*  
Photodeposition as a facile route to tunable Pt photocatalysts for  
hydrogen production: on the role of methanol

**175**  
YEARS



Cite this: *Catal. Sci. Technol.*, 2016,  
6, 81

## Photodeposition as a facile route to tunable Pt photocatalysts for hydrogen production: on the role of methanol†

Zhi Jiang,<sup>a</sup> ZheYu Zhang,<sup>a</sup> Wenfeng Shangguan,<sup>\*a</sup> Mark A. Isaacs,<sup>b</sup> Lee J. Durndell,<sup>b</sup> Christopher M. A. Parlett<sup>b</sup> and Adam F. Lee<sup>\*b</sup>

Photodeposition of H<sub>2</sub>PtCl<sub>6</sub> in the presence of methanol promotes the formation of highly dispersed, metallic Pt nanoparticles over titania, likely *via* capture of photogenerated holes by the alcohol to produce an excess of surface electrons for substrate-mediated transfer to Pt complexes, resulting in a high density of surface nucleation sites for Pt reduction. Photocatalytic hydrogen production from water is proportional to the surface density of Pt metal co-catalyst, and hence photodeposition in the presence of high methanol concentrations affords a facile route to optimising photocatalyst design and highlights the importance of tuning co-catalyst properties in photocatalysis.

Received 19th August 2015,  
Accepted 9th November 2015

DOI: 10.1039/c5cy01364j

[www.rsc.org/catalysis](http://www.rsc.org/catalysis)

### Introduction

Energy security and climate change represent key global challenges arising from historic reliance on fossil fuels.<sup>1–3</sup> Artificial photosynthesis offers the possibility of clean energy through water photolysis and renewable chemicals through CO<sub>2</sub> utilisation as a sustainable feedstock, commonly termed solar fuels and chemicals.<sup>4–7</sup> Hydrogen production through photocatalytic water splitting over semiconductor nanomaterials represents one of the most promising routes for the conversion and storage of solar energy in a form amenable for transportation.<sup>8–11</sup> Photoconversion efficiency is critically dependent upon the degree of charge separation and migration achievable in such semiconductors,<sup>12</sup> as well as the rate of subsequent surface catalysed reactions, properties which may be strongly influenced by the introduction of co-catalysts to the semiconductor surface.<sup>13–16</sup> Controlling the physicochemical properties of co-catalysts, and understanding how these impact upon subsequent photocatalytic reactions, is thus essential in order to advance the rational design of improved, high efficiency materials for water splitting. However, elucidating the key physicochemical properties of co-catalysts in water splitting and related photocatalytic transformations remains challenging. For example, metallic Pt nanoparticle co-catalysts have been previously reported as

either inferior,<sup>17–20</sup> or superior,<sup>21,22</sup> to electron rich/deficient Pt counterparts. Such inconsistencies may arise from the many differences in catalyst synthesis, which in turn may result in diverse nanoparticle size, dispersion, oxidation state and morphology. It is therefore highly desirable to develop synthetic routes capable of independently tuning the chemical state or particle size of such co-catalysts in order to definitively determine the key factors influencing Pt co-catalyst promotion and thereby optimise photocatalyst performance.

We recently demonstrated an *in situ* polyol method as one route to the preparation of well-defined hybrid photocatalysts,<sup>23,24</sup> however removal of the resultant ligands, long timescale, and poor cost efficiency for such a process remain problematic. Photodeposition (PD) offers an atom efficient and energy efficient versatile alternative method to introduce noble metal co-catalysts to semiconductor surfaces,<sup>25</sup> although to date it has afforded poor control over properties of the deposited co-catalyst.<sup>25,26</sup> Previous studies on the photodeposition of Pt over titania have focused on the development of novel molecular precursors, such as Pt(dcbpy)Cl<sub>2</sub>,<sup>27</sup> or the loading/time-dependent evolution of platinum species<sup>28–30</sup> and their reactivity for hydrogen production or methanol oxidation. In all cases, PD was performed in the presence of a fixed alcohol concentration to assist platinum reduction, typically 5–20 vol% methanol, although Ma *et al.* noted small differences in the size of Pt nanoparticles between 2 M methanol, ethanol and isopropanol.<sup>28</sup> However, the influence of alcohol concentration on the PD process and resulting photoactivity has never been explored to date. Here we demonstrate the critical role of methanol in tuning the oxidation state and dispersion of Pt nanoparticles during their PD from aqueous chloroplatinic

<sup>a</sup> Research Center for Combustion and Environment Technology, Shanghai Jiao Tong University, Shanghai, 200240, China. E-mail: [shangguan@sjtu.edu.cn](mailto:shangguan@sjtu.edu.cn); Tel: +86 21 34206020

<sup>b</sup> European Bioenergy Research Institute, Aston University, Birmingham, UK. E-mail: [a.f.lee@aston.ac.uk](mailto:a.f.lee@aston.ac.uk); Tel: +44 (0)1204 4036

† Electronic supplementary information (ESI) available: Details of experimental, data of XRD, XPS, TEM, XAFS. See DOI: 10.1039/c5cy01364j







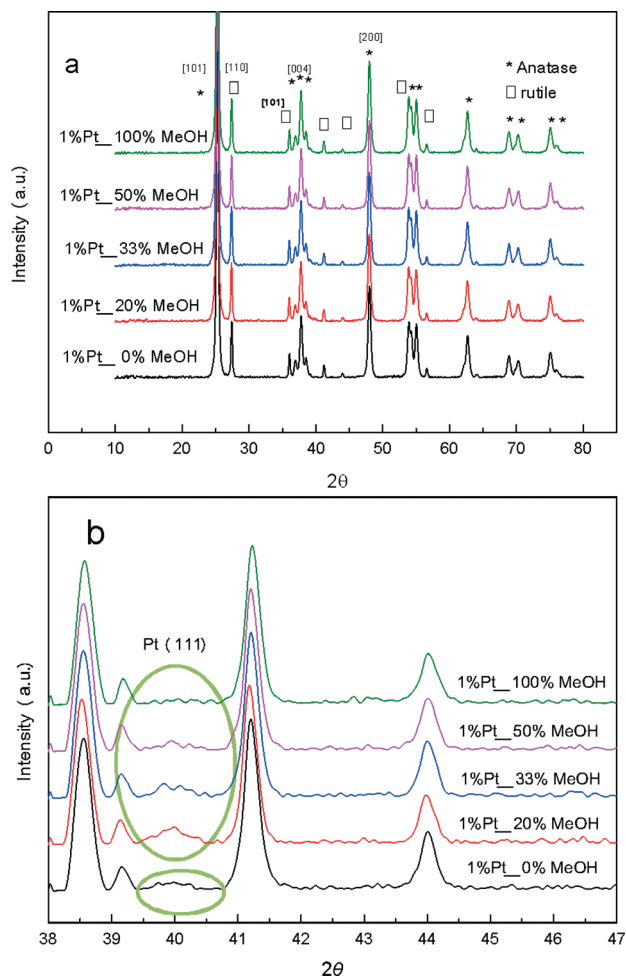


Fig. 2 (a) Wide angle and (b) high resolution XRD patterns of 1 wt% Pt/TiO<sub>2</sub> catalysts as a function of methanol concentration during PD.

Table 1 Structural properties of 1 wt% Pt/TiO<sub>2</sub> catalysts

Sample	Pt loading <sup>a</sup> /wt%	BET surface area <sup>b</sup> /m <sup>2</sup> g <sup>-1</sup>	Anatase particle size <sup>c</sup> /nm	Rutile particle size <sup>c</sup> /nm
P25	—	50	21.5	32.9
0% MeOH	1.01	51	22.0	34.6
20% MeOH	1.04	52	21.6	32.7
33% MeOH	1.04	50	21.0	31.1
50% MeOH	1.11	50	21.7	32.5
100% MeOH	1.04	49	21.3	32.5

<sup>a</sup> ICP-AES elemental analysis. <sup>b</sup> N<sub>2</sub> porosimetry. <sup>c</sup> XRD line broadening.

catalyst species formed during PD, or associated interfacial interaction between co-catalyst and titania.

High resolution XRD of the PD synthesised catalysts revealed the presence of a weak, broad peak around 39.8° corresponding to fcc platinum metal for the MeOH-20% and

MeOH-33% materials (Fig. 2b), whose intensity decreased with increasing MeOH concentration during PD. Surprisingly, this feature was absent for Pt/TiO<sub>2</sub> prepared with pure water or pure methanol. Since all catalysts contained the same amount of platinum, and there was no evidence for crystalline Pt oxide phases, the loss of a metallic Pt feature with MeOH concentration could reflect a decrease in nanoparticle size, with the MeOH-0% and MeOH-100% materials containing either small metal (or potentially oxide or mono-nuclear Pt complexes) below the sensitivity limit. This hypothesis is supported by HRTEM (Fig. 3) and H<sub>2</sub> chemisorption (Fig. S2<sup>†</sup>), which revealed highly dispersed Pt nanoparticles with diameters <2.5 nm for the MeOH-100% and MeOH-0% materials, in contrast to the MeOH-20% material which contained larger (>4 nm) Pt nanoparticles. Lattice fringes characteristic of fcc Pt metal were observable for all samples photodeposited in the presence of methanol. While a small number of Pt containing particles were observed at the interface of between titania crystallites (Fig. 3d), in general they appeared randomly distributed across the surfaces of both anatase and rutile crystallites (Fig. 3 and S3<sup>†</sup>). The Pt co-catalyst oxidation state was investigated by XPS (Fig. 4), with Pt 4f XP spectra revealing the co-existence of spin-orbit split doublets associated with Pt metal (4f<sub>7/2</sub> = 70.4 eV binding energy), PtCl<sub>x</sub> from the parent chloroplatinic acid (4f<sub>7/2</sub> = 71.9 eV), and PtO<sub>2</sub> (4f<sub>7/2</sub> = 73.3 eV). The catalyst prepared in the absence of MeOH during PD comprised predominantly oxide and PtCl<sub>x</sub>, the latter consistent with the presence of a Cl 2p peak (Fig. S4<sup>†</sup>, not observed for other catalysts) and the lack of Pt metal reflections by XRD. Corresponding O 1s XP spectra were dominated by the titania substrate, revealing only a single state at 529.8 eV (Fig. S5<sup>†</sup>) consistent with TiO<sub>2</sub> independent of methanol concentration.<sup>33</sup> Despite previous reports that photodeposition in the absence of an electron donor<sup>34</sup> affords platinized-TiO<sub>2</sub> containing mainly PtO<sub>x</sub>, we observe the co-existence of significant PtCl<sub>x</sub> and (highly dispersed) PtO<sub>2</sub> under such conditions (Fig. 5a). The proportion of Pt metal and PtCl<sub>x</sub> precursor/PtO<sub>2</sub> exhibit a striking switchover from electron-deficient → metallic platinum upon methanol introduction during PD. This is accompanied by an initial drop in the overall Pt:Ti surface atomic ratio between MeOH-0% and MeOH-20% (Fig. 5b) indicating a decrease in Pt dispersion, and subsequent monotonic rise associated with an increase in Pt dispersion. The Pt:Ti surface atomic ratios also demonstrate that the surface coverage of Pt nanoparticles decorating the titania support varies between 0.33 and 0.5 of a monolayer with increasing methanol concentration. These observations are consistent with the presence of the parent PtCl<sub>x</sub> precursor, and a high density of small *oxidic* Pt nanoparticles dispersed across titania when PD was conducted without methanol, and genesis of large *metallic* Pt particles on introducing a low concentration of methanol, which shrink *but remain metallic* as the methanol concentration rises. Methanol thus drives both platinum reduction and its subsequent redispersion, such that the surface density of Pt<sup>0</sup> species increases continuously with the concentration of



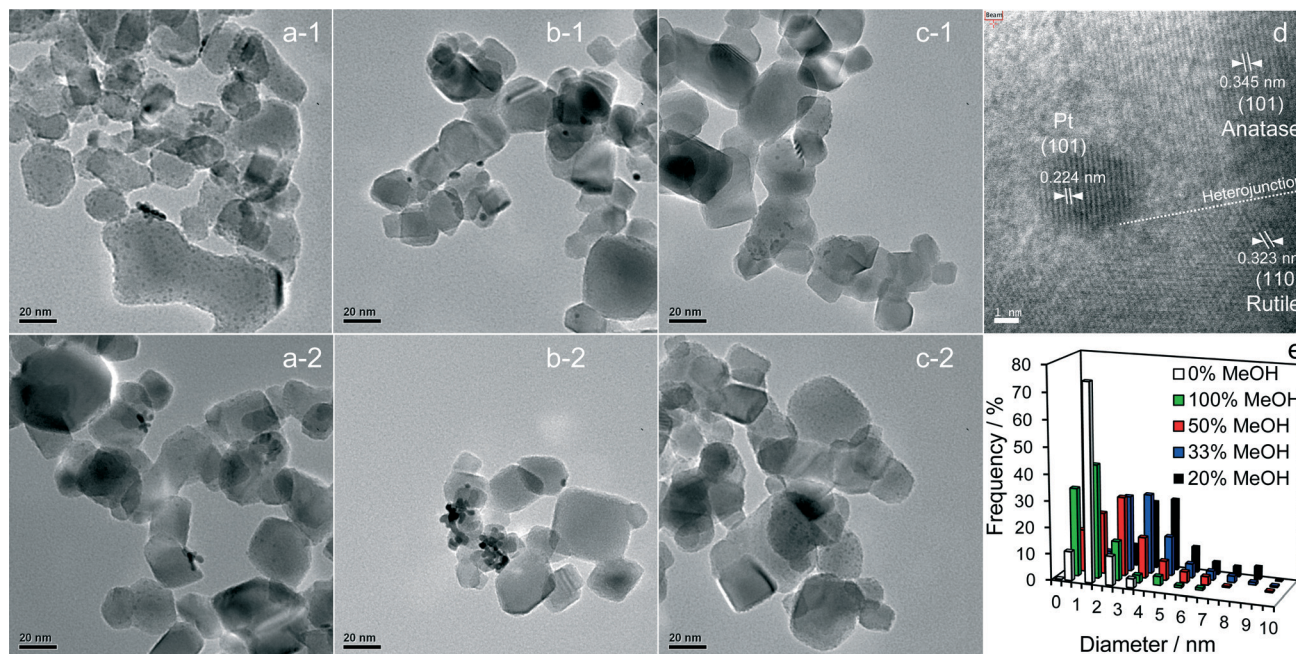


Fig. 3 Representative bright-field HRTEM images of (a1–2) 100%, (b1–2) 20%, and (c1–2) 0% MeOH 1 wt% Pt/TiO<sub>2</sub>, (d) an individual Pt metal nanoparticle at the interface between anatase and rutile crystallites, and (e) particle size distributions as a function of methanol concentration during PD.

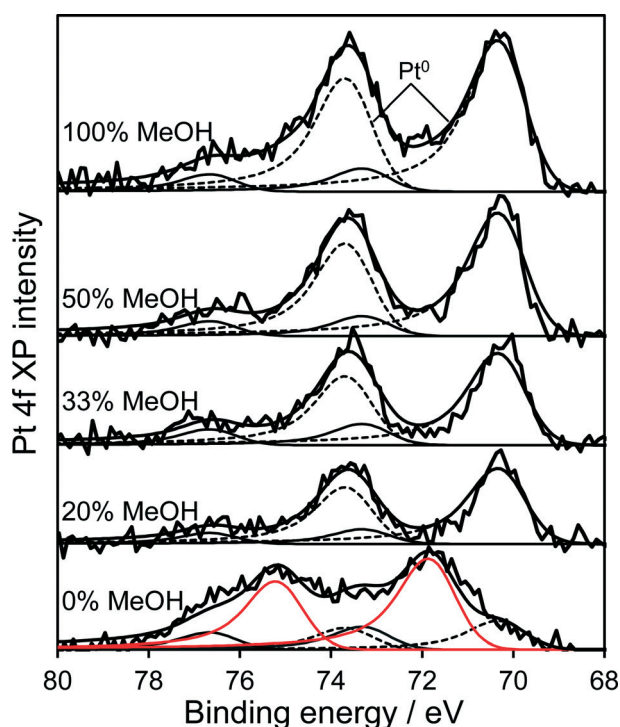


Fig. 4 Pt 4f XPS spectra of 1 wt% Pt/TiO<sub>2</sub> catalysts as a function of methanol concentration during PD.

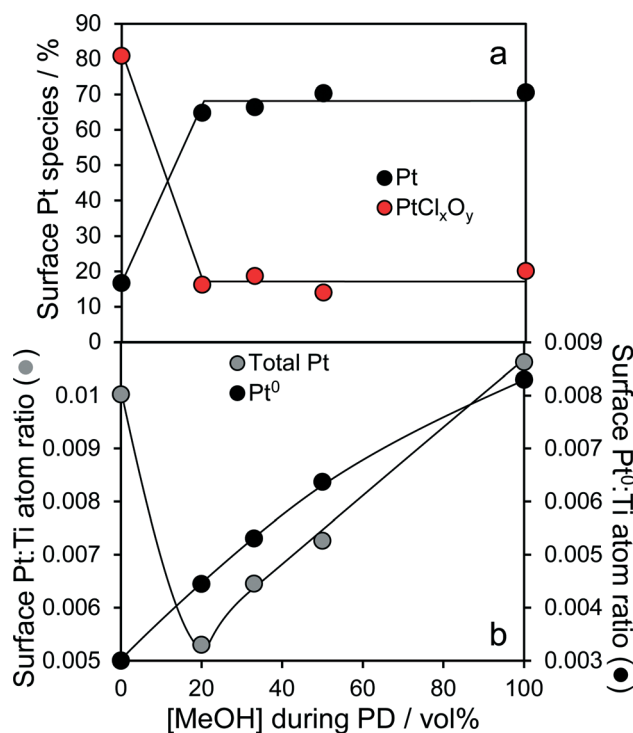


Fig. 5 (a) Evolution of platinum surface oxidation state, and (b) relative dispersion of total and metallic platinum for 1 wt% Pt/TiO<sub>2</sub> catalysts as a function of methanol concentration during PD.

methanol during PD (Fig. 5b). It is important to note that this increase in surface metal occurs in parallel with the loss of corresponding XRD features, confirming that high methanol concentrations indeed promote Pt dispersion as small, metallic nanoparticles. The rise in surface Pt<sup>0</sup> between M-20% and M-100% does not quantitatively match the

associated 61% increase in H<sub>2</sub> productivity, indicating a more significant role for co-catalyst particle size effects in photoactivity than previously reported.<sup>35</sup>

Pt L<sub>III</sub>-edge XAS of the co-catalyst (Fig. 6a) reveal that normalised XANES spectra of MeOH-20% and MeOH-100%







Table 2 Pt L<sub>III</sub>-edge EXAFS fitted parameters

Sample	CN1 <sup>a</sup> Pt–Pt	CN2 Pt–Pt	CN3 Pt–Pt	CN1 Pt–O	CN2 Pt–O	CN3 Pt–Pt	Amplitude factor
Pt foil	12	6	24	—	—	—	0.9037
100% MeOH	7.6	1.0	3.1	—	—	—	0.9037/0.7933
20% MeOH	8.5	1.7	3.6	—	—	—	0.9037/0.7933
0% MeOH	1.5	—	—	1.2	2.1	1.3	0.9037/0.7933
PtO <sub>2</sub>	—	—	—	2	4	2	0.7933
Sample	R1 <sup>b</sup> Pt–Pt	R2 Pt–Pt	R3 Pt–Pt	R1 Pt–O	R2 Pt–O	R1 Pt–Pt	
Pt foil	2.76	3.91	4.79	—	—	—	
100% MeOH	2.75	3.89	4.77	—	—	—	
20% MeOH	2.76	3.91	4.78	—	—	—	
0% MeOH	2.76	—	—	1.94	2.05	3.15	
PtO <sub>2</sub>	—	—	—	1.92	2.02	3.14	
Sample	σ1 <sup>c</sup> Pt–Pt	σ2 Pt–Pt	σ3 Pt–Pt	σ2 Pt–O	σ2 Pt–O	R-factor %	
Pt foil	0.005	0.006	0.007	—	—	3.18	
100% MeOH	0.005	0.005	0.006	—	—	4.09	
20% MeOH	0.005	0.006	0.006	—	—	3.57	
0% MeOH	0.004	—	—	0.007	0.007	6.19	
PtO <sub>2</sub>	—	—	—	0.006	0.003	4.78	

<sup>a</sup> Coordination number. <sup>b</sup> Interatomic scattering distance. <sup>c</sup> Debye–Waller factor.

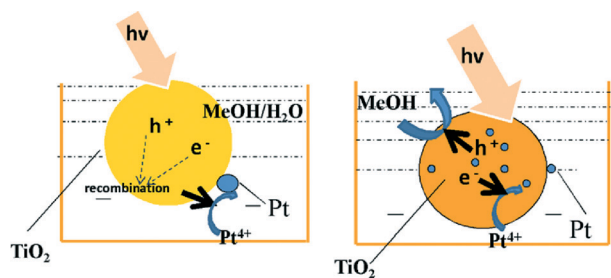


Fig. 7 Schematic of the proposed mechanism for methanol-promoted PD of highly dispersed platinum nanoparticles over titania.

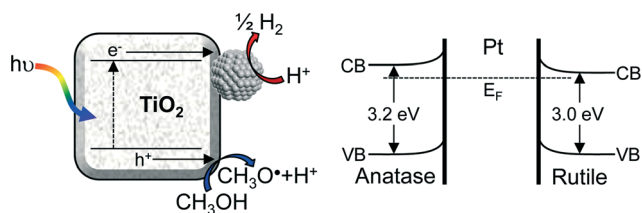


Fig. 8 Schematic of photocatalytic hydrogen production via exciton creation and charge separation between highly dispersed platinum nanoparticles and titania.

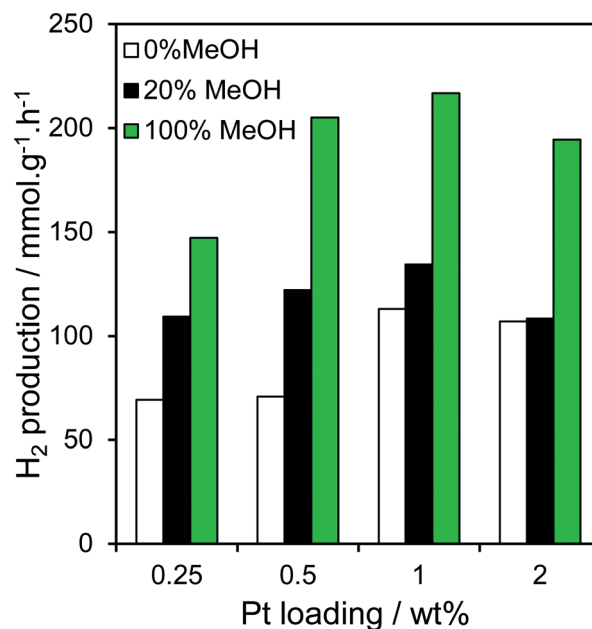


Fig. 9 Photocatalytic hydrogen evolution over Pt/TiO<sub>2</sub> catalysts as a function of Pt loading and methanol concentration during PD.

relationship between [MeOH] during PD and photoactivity observed in Fig. 1 appears related to the surface Pt<sup>0</sup>:Ti atomic ratio (from XPS) shown in Fig. 5b, indicating that hydrogen production scales with the interfacial contact area between titania and Pt metal. This relationship is highlighted

in Fig. 10 and appears loading independent, offering a simple spectroscopic method by which to quantitatively predict the photocatalytic performance of Pt/TiO<sub>2</sub> in hydrogen production.

Considering that the co-catalyst physical and electronic properties are so important in this reaction, one must







- 27 R. S. Khnayzer, L. B. Thompson, M. Zamkov, S. Ardo, G. J. Meyer, C. J. Murphy and F. N. Castellano, *J. Phys. Chem. C*, 2012, **116**, 1429–1438.
- 28 J. Ma, E. Valenzuela, A. S. Gago, J. Rousseau, A. Habrioux and N. Alonso-Vante, *J. Phys. Chem. C*, 2014, **118**, 1111–1117.
- 29 L. M. Ahmed, I. Ivanova, F. H. Hussein and D. W. Bahnemann, *Int. J. Photoenergy*, 2014, **2014**, 9.
- 30 M. Kim, A. Razzaq, Y. K. Kim, S. Kim and S.-I. In, *RSC Adv.*, 2014, **4**, 51286–51293.
- 31 M. D. Driessen and V. H. Grassian, *J. Phys. Chem. B*, 1998, **102**, 1418–1423.
- 32 W. Zhao, C. Chen, X. Li, J. Zhao, H. Hidaka and N. Serpone, *J. Phys. Chem. B*, 2002, **106**, 5022–5028.
- 33 V. N. I. o. S. a. T., *NIST X-ray Photoelectron Spectroscopy Database*, Gaithersburg, 2012, <http://srdata.nist.gov/xps/>.
- 34 T. Sano, N. Negishi, K. Uchino, J. Tanaka, S. Matsuzawa and K. Takeuchi, *J. Photochem. Photobiol., A*, 2003, **160**, 93–98.
- 35 J. Lee and W. Choi, *J. Phys. Chem. B*, 2005, **109**, 7399–7406.
- 36 A. I. Frenkel, C. W. Hills and R. G. Nuzzo, *J. Phys. Chem. B*, 2001, **105**, 12689–12703.
- 37 A. L. Linsebigler, G. Lu and J. T. Yates, *Chem. Rev.*, 1995, **95**, 735–758.
- 38 D. C. Hurum, A. G. Agrios, K. A. Gray, T. Rajh and M. C. Thurnauer, *J. Phys. Chem. B*, 2003, **107**, 4545–4549.
- 39 G. Li, S. Ciston, Z. V. Saponjic, L. Chen, N. M. Dimitrijevic, T. Rajh and K. A. Gray, *J. Catal.*, 2008, **253**, 105–110.
- 40 M. A. Henderson, *Surf. Sci. Rep.*, 2011, **66**, 185–297.
- 41 H. Xu, G. Li, G. Zhu, K. Zhu and S. Jin, *Catal. Commun.*, 2015, **62**, 52–56.

